Anti-silencing function 1B promotes the progression of pancreatic cancer by activating c-Myc

MIN ZHANG[1], LUYANG ZHANG[1], MINGHE ZHOU[1], ENZE WANG[1], BO MENG[1], QINGJUN LI[1], XIAOQIAN WANG[1], YUNJIAN WANG[1] and QIONG LI[2]

[1]Department of Hepatobiliary and Pancreatic Surgery, The Affiliated Cancer Hospital of Zhengzhou University, Zhengzhou, Henan 450008; [2]Key Laboratory for Medical Tissue Regeneration of Henan Province, Xinxiang Medical College, Xinxiang, Henan 453003, P.R. China

Received June 16, 2022; Accepted August 31, 2022

DOI: 10.3892/ijo.2022.5456

Abstract. The present study aimed to explore the role of histone chaperone anti-silencing function 1B (ASF1B) in pancreatic cancer and the underlying mechanism. The biological function of ASF1B was investigated in pancreatic cancer cell lines (PANC-1 and SW1990) and a mouse xenograft model. Chromatin immunoprecipitation was used to detect the effect of ASF1B on the transcriptional activity of c-Myc. ASF1B was highly expressed in pancreatic adenocarcinoma (PAAD) samples from The Cancer Genome Atlas. ASF1B expression was positively associated with poor survival rates in patients with PAAD. Silencing of ASF1B in PANC-1 and SW1990 cells inhibited cell proliferation, migration and invasion, and induced apoptosis. Mechanistically, ASF1B increased H3K56 acetylation (H3K56ac) in a CREB-binding protein (CBP)-dependent manner. ASF1B promoted H3K56ac at the c-Myc promoter and increased c-Myc expression. In PANC-1 and SW1990 cells, the CBP inhibitor curcumin and the c-Myc inhibitor 10058-F4 reversed the promoting effects of ASF1B on cell proliferation, migration and invasion. In the mouse xenograft model, ASF1B silencing inhibited tumor growth, and was associated with low H3K56ac and c-Myc expression. ASF1B promoted pancreatic cancer progression by activating c-Myc via CBP-mediated H3K56ac.

Correspondence to: Dr Yunjian Wang, Department of Hepatobiliary and Pancreatic Surgery, The Affiliated Cancer Hospital of Zhengzhou University, 127 Dongming Road, Jinshui, Zhengzhou, Henan 450008, P.R. China
E-mail: hnszlyywyj@sina.com

Dr Qiong Li, Key Laboratory for Medical Tissue Regeneration of Henan Province, Xinxiang Medical College, 601 Jinsui Avenue, Hongqi, Xinxiang, Henan 453003, P.R. China
E-mail: aprilliqiong@163.com

Abbreviations: ASF1B, anti-silencing function 1B; CBP, CREB-binding protein; H3K56ac, histone H3 lysine 56 acetylation; PAAD, pancreatic adenocarcinoma; TCGA, The Cancer Genome Atlas

Key words: pancreatic cancer, ASF1B, c-Myc, H3K56 acetylation, CBP

Introduction

Pancreatic cancer is one of the most common digestive system malignancies with a 5-year survival rate of 9% in 2008-2014 in the United States (1). At present, surgery is the most efficient therapy for pancreatic cancer; however, only ~20% of patients are diagnosed with surgically resectable disease (2). Furthermore, metastasis occurs in patients undergoing extensive resection (3,4). Metastatic response and progression of pancreatic cancer contribute to poor clinical outcomes (5). The pathogenesis of pancreatic cancer is complicated and involves various processes and signaling pathways (6,7). It is a priority to understand the mechanisms underlying the development and progression of pancreatic cancer.

Anti-silencing function 1 (ASF1) comprises two subtypes, ASF1A and ASF1B, which share a 70% sequence homology (8,9). ASF1B is a histone H3/H4 chaperone involved in DNA repair, replication and transcriptional regulation (10). ASF1B controls chromatin function and has been demonstrated to participate in tumorigenesis (11). Previous studies have determined that ASF1B is closely associated with the development and progression of numerous cancer types, such as prostate, breast and cervical cancer (12,13). In addition, ASF1B is frequently highly expressed in pancreatic cancer specimens and is closely associated with poor prognosis (14). Inhibition of ASF1B in pancreatic cancer cells enhances cisplatin sensitivity, inhibits micrometastasis and results in tumor cell death (14,15). In addition, c-Myc serves as an essential cancer-related transcription factor involved in diverse critical biological processes of cancer development (16-18). c-Myc has been reported to serve a critical role in modulating pancreatic cancer progression (19,20); however, the association between c-Myc and ASF1B in the modulation of pancreatic cancer progression remains unclear.

Epigenetic regulation serves as a program by which gene expression is modulated by events other than genomic alterations (21). Due to the extensive effect of epigenetic regulation on gene expression and genomic stability, it serves a fundamental role in a number of physiological and

pathological processes, and influences carcinogenesis from initiation to progression (22), thus serving as a potential driver of tumorigenesis (21,23). As a common epigenetic regulator, histone acetylation serves a crucial role in the modulation of cancer development (24). Furthermore, it has been reported that ASF1 promotes anti-viral immune activity by associating with CREB-binding protein (CBP) to mediate H3K56 acetylation (H3K56ac) at the promoter of interferon β (25). Multi-site substrate recognition in ASF1-related histone H3K56ac through regulator of Ty1 transposition 109 has also been identified (26). CBP is an essential transcriptional co-activator for a number of DNA-binding transcription factors and acts as a histone acetyltransferase (27). The CBP-mediated acetylation of H3K56 is involved in the modulation of cell proliferation and cancer (28). However, the association of ASF1B with CBP and H3K56ac in the development of pancreatic cancer remains elusive.

The present study aimed to explore the role and the underlying mechanism of ASF1B in the modulation of pancreatic cancer. The present study revealed that ASF1B promoted pancreatic cancer progression by activating c-Myc through CBP-mediated H3K56ac.

Materials and methods

Clinical pancreatic cancer samples. A total of 31 clinical pancreatic cancer samples were obtained from the Cancer Hospital Affiliated to Zhengzhou University (Zhengzhou, China) between May 2019 and December 2020. Clinicopathological information of patients is shown in Table I. The inclusion criteria were: Patients were diagnosed by clinical and pathological examination by two clinicians; no systemic or local therapy was administered before the surgery; and written informed consent was obtained from each patient before using the collected samples. The exclusion criteria were: Patients with cirrhosis and coagulation dysfunction; patients with serious cardiovascular and visceral diseases; patients with a history of second primary malignant tumors; and patients with mental illness or confused consciousness. The present study included 19 male and 12 female patients with an age range of 49-75 years (median age, 63.45±7.54 years). The pancreatic cancer tissues and corresponding para-neoplastic tissues obtained from the patients were immediately frozen in liquid nitrogen, followed by storage at -80˚C prior to further analysis. The present study was performed in accordance with the World Medical Association guidelines and approved by the Ethics Committee of Cancer Hospital Affiliated to Zhengzhou University (Ethics No. 2019-05-006; Zhengzhou, China).

Bioinformatics analysis. The data for ASF1B mRNA expression in pancreatic cancer and normal specimens were from Gene Expression Profiling Interactive Analysis (GEPIA) (29) (http://gepia.cancer-pku.cn/). The Cancer Genome Atlas (TCGA; ID, TCGA-PAAD; https://portal.gdc.cancer.gov/) data were used for GEPIA. According to ASF1B expression, the top and bottom 25% patients with pancreatic cancer were divided into high and low expression groups. The overall survival of 90 patients with pancreatic cancer was estimated using GEPIA with a cutoff value of 25%. Kaplan-Meier analysis was used for analyzing the difference of overall survival between the high and low expression groups using the log-rank test. Gene Set Enrichment Analysis (GSEA; version 4.2.1; h.all.v7.1.symbols.gmt; https://www.gsea-msigdb.org/gsea/index.jsp) was performed using R (version 3.4.1; https://cran.r-project.org/index.html) and the R clusterProfiler package (Bioconductor version 3.10; http://www.bioconductor.org/packages/3.10/bioc/html/clusterProfiler.html) (30) to explore signaling pathways.

Cell culture. PANC-1 (cat. no. CL-0184), CFPAC-1 (cat. no. CL-0059), PaCa-2 (cat. no. CL-0627) and HPAF-II (cat. no. CL-0611) pancreatic adenocarcinoma (PAAD) cell lines were purchased from Procell Life Science & Technology Co., Ltd., and the SW1990 (cat. no. CRL-2172) cell line was purchased from American Type Culture Collection. PANC-1 and SW1990 cells exhibiting epithelial morphology were used throughout the study. PANC-1 cells were cultured in DMEM (cat. no. 11965092; Gibco; Thermo Fisher Scientific, Inc.) supplemented with 10% FBS (cat. no. SH30406.02; HyClone; Cytiva) and 1% penicillin-streptomycin solution (Beyotime Institute of Biotechnology). SW1990 cells were cultured in Leibovitz's L-15 medium (cat. no. 30-2008; American Type Culture Collection) supplemented with 10% FBS and 1% penicillin-streptomycin solution. CFPAC-1 cells were cultured in Iscove's Modified Dulbecco Medium (Procell Life Science & Technology Co., Ltd.) supplemented with 10% FBS and 1% penicillin-streptomycin solution. PaCa-2 cells were cultured in DMEM supplemented with 10% FBS, 2.5% horse serum (Procell Life Science & Technology Co., Ltd.) and 1% penicillin-streptomycin solution. HPAF-II cells were cultured in Minimum Essential Medium (Procell Life Science & Technology Co., Ltd.) supplemented with 10% FBS and 1% penicillin-streptomycin solution. All cell lines were maintained at 37˚C in a 5% CO_2 air atmosphere and 100% air, respectively.

The CBP inhibitor curcumin and c-Myc inhibitor 10058-F4 were purchased from MedChemExpress. Curcumin and 10058-F4 were used to treat cells at a concentration of 100 μM for 24 h at 37˚C.

Plasmids, small interfering RNA (siRNA/si) and transfection. To construct Flag-tagged ASF1B, total RNAs was extracted from PANC-1 cells using TRIzol (Invitrogen; Thermo Fisher Scientific, Inc.). The full coding region of the ASF1B gene was obtained by PCR with the specific primers of forward, 5'-CCC AAGCTTATGGCCAAGGTGTCGGTGCT-3' (*Hin*dIII) and reverse, 5'-CGGGATCCTTAGATGCAGTCCATGGAGT-3' (*Bam*HI) using PrimeSTAR HS DNA Polymerase (Takara Biotechnology Co., Ltd.). The thermocycling conditions were: 98˚C for 10 sec, followed by 30 cycles of 55˚C for 5 sec and 72˚C for 1 min. The PCR products were ligated into the p3XFLAG-CMV™-14 expression vector (MilliporeSigma) using the In-Fusion HD Cloning Kit (Takara Biotechnology Co., Ltd.). Empty vector was used as the negative control. siRNAs specific for ASF1B and CBP, and the non-targeting negative controls were obtained from TsingKe Biological Technology. The *Homo sapiens* siRNA sequences were as follows: si-ASF1B-1, 5'-GTTCATCCGAGTGGGCTA CTA-3'; si-ASF1B-2, 5'-GGTGACCCGCTTCCATAT

Table I. Clinicopathological information of patients with pancreatic cancer.

Variables	Cases, n (%)
Sex	
Male	19 (61.29)
Female	12 (38.71)
Age, years	
≤60	10 (32.26)
>60	21 (67.74)
Histopathology	
Ductal adenocarcinoma	22 (70.97)
Other	9 (29.03)
Location	
Head of pancreas	23 (74.19)
Other	8 (25.81)
Grade	
G1	2 (6.45)
G2	11 (35.48)
G3	18 (58.06)
Stage	
I	4 (12.90)
II	9 (29.03)
III	17 (54.84)
IV	1 (3.23)

CAA-3'; and si-CBP, 5'-GCAAGTCATGAATGGATCTCT-3'. Non-targeting siRNAs were used as negative controls (siNC): 5'-GCTCGTAAGCGTAGGTCTTCA-3' (for si-ASF1B-1 and si-ASF1B-2); 5'-GCTTAAGATGACGCAGTTCTA-3' (for si-CBP). Cells were transfected with vectors (2 μg for '+' group and 5 μg for '++' group) or siRNAs (100 nM) using Lipofectamine 3000 (Invitrogen; Thermo Fisher Scientific, Inc.) for 48 h at 37˚C according to the manufacturer's instructions. The time interval between transfection and subsequent experimentation was <1 week.

Cell Counting Kit-8 (CCK-8) assay. Following transfection, PANC-1 and SW1990 cells (1x10^5 cells/well) were plated in 96-well plates and cultured for 0-72 h. Cell proliferation was measured using 10 μl/well CCK-8 (Dojindo Molecular Technologies, Inc.) for 2 h at 37˚C. The optical density value at 450 nm was measured using an ELISA reader (Bio-Tek EL 800; BioTek Instruments, Inc.).

Colony formation. Following transfection with siRNAs, empty vector or flag-tagged ASF1B, PANC-1 and SW1990 cells (1,000 cells/well) were plated in 6-well plates and treated with 100 μM curcumin or 100 μM 10058-F4 for 24 h at 37˚C. Non-treated cells were used as the control group. The culture medium was replaced every 3 days. Colonies were washed twice with PBS, fixed with 4% paraformaldehyde for 30 min at room temperature and stained with 0.5% crystal violet (Beyotime Institute of Biotechnology) for 1 h at room temperature, and images were captured. Colonies with at least 50 cells were counted using ImageJ software (version 5.0; National Institutes of Health).

Cell apoptosis detection. Following transfection, PANC-1 and SW1990 cells (2x10^5 cells/well) were plated in 6-well dishes. After 48 h, apoptotic cells were stained using the Annexin V-FITC Early Apoptosis Detection Kit (Cell Signaling Technology, Inc.) according to the manufacturer's instructions. Apoptotic cells were analyzed using flow cytometry (Accuri-C6 plus; BD Biosciences). The number of apoptotic cells was analyzed using FlowJo software (v7.6.5; Tree Star, Inc.).

Transwell assays. For cell migration assays, 1x10^5 transfected PANC-1 and SW1990 cells were placed in the upper chamber of a Corning® FluoroBlok™ 24-well Transwell system (Costar; Corning, Inc.). The cells in the upper chamber were maintained in DMEM or Leibovitz's L-15 base medium without serum. The lower chamber was filled with DMEM or Leibovitz's L-15 medium supplemented with 10% FBS. After 12 h of incubation at 37˚C, the cells that had migrated into the lower chamber were fixed with 4% paraformaldehyde for 30 min at room temperature and stained with 0.5% crystal violet (Beyotime Institute of Biotechnology) for 30 min at room temperature. For cell invasion assays, the Transwell system was pre-coated with 100 μl Matrigel (Invitrogen; Thermo Fisher Scientific, Inc.) for 4 h at 37˚C. The other steps were the same as for the migration assay. Images were captured under a light microscope (Eclipse 80i; Nikon Corporation). The migrated and invaded cells in five randomly selected fields of view in the lower chamber were counted to calculate cell migration and invasion. Both the migration and invasion assays were performed in triplicate.

Scratch test. Following transfection, PANC-1 and SW1990 cells (3x10^5 cells/well) were plated overnight in 24-well dishes to reach full confluence as a monolayer. A 20-μl pipette tip was used to create a scratch across the well. Floating cells were removed by washing three times with PBS. The cultures were maintained at 37˚C for 6 or 12 h in serum-free culture medium, and then images were captured under a light microscope (Eclipse 80i; Nikon Corporation). The wound distance was measured using ImageJ software (version 5.0; National Institutes of Health).

Reverse transcription-quantitative PCR (RT-qPCR). Total RNAs was extracted from the human specimens and PANC-1 and SW1990 cell lines using TRIzol (Invitrogen; Thermo Fisher Scientific, Inc.). First-strand cDNA was synthesized using the PrimeScript™ RT Master Mix (cat. no. RR036A; Takara Biotechnology Co., Ltd.). The reverse transcription conditions were 37˚C for 15 min followed by 85˚C for 5 sec. qPCR was performed using the TB Green Fast qPCR Mix (cat. no. RR430A; Takara Biotechnology Co., Ltd.). Relative expression of the target genes was calculated according to the $2^{-\Delta\Delta Cq}$ method by normalizing to the β-actin internal control (31). The *Homo sapiens* primer sequences were as follows: ASF1B forward, 5'-GATCAGCTTCGAGTGCAG TG-3' and reverse, 5'-TGGTAGGTGCAGGTGATGAG-3'; c-Myc forward, 5'-GGCTCCTGGCAAAAGGTCA-3' and reverse, 5'-CTGCGTAGTTGTGCTGATGT-3'; and β-actin forward, 5'-GATTCCTATGTGGGCGACGA-3' and reverse,

5'-CACAGGACTCCATGCCCAG-3'. The thermocycling conditions were: 95˚C for 30 sec, followed by 40 cycles of 95˚C for 5 sec and 60˚C for 10 sec.

Western blot analysis. Total proteins were extracted from the collected tissue samples and cell lines using RIPA buffer (Cell Signaling Technology, Inc.). Protein concentrations were measured using the BCA Protein Quantification Kit (Abbkine Scientific Co., Ltd.). Equal amounts (30 μg/lane) of protein extracts were subjected to 10-12% SDS-PAGE and transferred to PVDF membranes (MilliporeSigma). The membranes were blocked in 5% skimmed milk for 1 h at 37˚C. Membranes were incubated with primary antibodies against ASF1B (dilution, 1:1,000; cat. no. ab235358; Abcam), Bax (dilution, 1:1,000; cat. no. ab32503; Abcam), Bcl-2 (dilution, 1:1,000; cat. no. ab182858; Abcam), c-Myc (dilution, 1:1,000; cat. no. ab10910; Abcam), β-actin (dilution, 1:1,000; cat. no. ab8226; Abcam), H3 (dilution, 1:1,000; cat. no. ab1791; Abcam) and H3K56ac (dilution, 1:1,000; cat. no. PA5-121083; Thermo Fisher Scientific, Inc.) overnight at 4˚C. The membranes were then incubated with goat anti-rabbit (cat. no. ab7090), anti-mouse (cat. no. ab97040) and anti-rat (cat. no. ab7097) IgG H&L (HRP) secondary antibodies (dilution, 1:1,000; Abcam) for 1 h at room temperature. The bands were developed using BeyoECL Plus (Beyotime Institute of Biotechnology) and semi-quantified using ImageJ software (version 5.0; National Institutes of Health). To determine the protein half-life curves, the cells were treated with 25 μg/ml cycloheximide (CHX; MilliporeSigma) for 0-4 h at 37˚C.

Chromatin immunoprecipitation (ChIP). ChIP was performed using a SimpleChIP Enzymatic Chromatin IP Kit (Cell Signaling Technology, Inc.) according to the manufacturer's instructions. Following transfection with si-ASF1B-2 or siNC, cells were incubated with 1% formaldehyde for 15 min at room temperature, washed twice with PBS, centrifuged at 500 x g for 10 min at 4˚C, and collected in SDS lysis buffer (Beyotime Institute of Biotechnology). Chromatin prepared from the cells in a 15-cm dish was used to determine total DNA input and was incubated overnight with 10 μg anti-H3K56ac (cat. no. PA5-121083; Thermo Fisher Scientific, Inc.) or anti-IgG (cat. no. ab171870; Abcam) at 4˚C. In each immunoprecipitation, 10 μg of the protein-chromatin complex was used. Following incubation with 70 μl protein G agarose beads (Upstate Biotechnology, Inc.) for 2 h at 4˚C. The immune complexes were precipitated at 3,400 x g for 1 min at 4˚C and washed with 1 ml low salt washing solution. After three washes of low salt, 1 ml high salt solution was added to the beads and incubated at 4˚C for 5 min. The protein G agarose beads were precipitated by centrifugation at 3,400 x g for 1 min at 4˚C and then the supernatant was used in the next step. The PCR procedure was performed as aforementioned with the following primer sequences for amplifying the c-Myc promoter: Forward, 5'-GTTTCAACTGTTCTCGTCGTT-3' and reverse, 5'-TTCTTGTCCATGCCATAACCC-3'.

Pancreatic cancer xenograft. A total of 10 male BALB/c nude mice (8 weeks old; 22±2 g; Jinan Pengyue Laboratory Animal Breeding Co., Ltd.) were divided into two groups (n=5 per group): Short hairpin RNA (sh)NC and shASF1B. All animal experiments in the present study were approved by the Ethics Committee of Cancer Hospital Affiliated to Zhengzhou University (Ethics No. 2019-05-006; Zhengzhou, China) and performed in accordance with the standards of Animal Care and Use and the Animal Welfare Act. The tumor volume limit (≤2 cm in any dimension) was the humane endpoint criterion for mouse euthanasia. Mice were raised in specific pathogen-free conditions with *ad libitum* access to food and water. Mice were kept at 22±2˚C in a humid environment (60±10%) with a 12/12 h light-dark cycle. After acclimatization for 1 week, $5x10^6$ PANC-1 cells in 150 μl PBS were injected subcutaneously into the right side of the anterior flank of nude mice to establish *in vivo* tumor models. PANC-1 cells were pre-infected with lentiviral vectors (MOI, 20; Shanghai GeneChem Co., Ltd.) containing shNC (5'-ACCTCGTTG TACGAGCGTCGGAACTATCAAGAGTAGTTCCGACGC TCGTACAACTT-3') or shASF1B (5'-ACCTCGATCAGC TTCGAGTGCAGTGATCAAGAGTCACTGCACTCGAAG CTGATCTT-3'). These sequences were cloned into the GV115 vector (Shanghai GeneChem Co., Ltd.) and the lentivirus was packaged in 293T cells. The third generation of 293T cells (The Cell Bank of Type Culture Collection of The Chinese Academy of Sciences) were inoculated into the 10-cm cell culture dish (Corning, Inc.). After 24 h, when the cell density reached 70-80%, the plasmids including 20 μg GV vector, 15 μg pHelper 1.0 and 10 μg pHelper 2.0 (the ratio was: 4:3:2) were transfected using Lipofactamine 3000 (Thermo Fisher Scientific, Inc.). The cells were cultured in the 5% CO_2 incubator at 37˚C for 48 h, then the cell supernatant was collected for subsequent experiments. After centrifugation at 25,000 x g for 2 h at 4˚C and filtration through 0.22-μm filters, lentiviral particles (MOI, 20) were transduced into PANC-1 cells for 24 h, the infected medium was replaced with fresh medium. After 72 h of continuous culture with puromycin (1 μg/ml) for stable cell line selection, cells were cultured with puromycin (0.5 μg/ml) for amplification. Subcutaneous inoculation was started after amplification. None of the mice died during the experimental procedures. From 10 days after the injection, the sizes of the subcutaneous tumors were measured on day 10, 12, 15, 17, 20, 22, 25, 27 and 30 using calipers. The tumor volumes were calculated and the results for day 10, 15, 20, 25 and 30 are presented. The length and width of the tumors were calculated using calipers. Tumor volume=(length x $width^2$)/2. At 30 days after injection, the mice were sacrificed by cervical dislocation with prior anesthesia by intraperitoneal injection of 3% sodium pentobarbital (30 mg/kg). Death was verified to be respiratory cardiac arrest for at least 10 min and the observation of pupil dilation. Tumor tissues were washed with ice-cold PBS, weighed and subjected to immunohistochemical staining.

Histological examination. Human para-neoplastic and pancreatic cancer tissues were subjected to immunohistochemical staining. Tumor tissues were collected from the xenograft mouse model. Tissues were sliced (thickness, 0.1 mm) and then fixed with 4% paraformaldehyde at 4˚C for 2 h, permeabilized in 0.5% Triton X-100 at room temperature for 10 min and coated with paraffin. Tissue sections were heated at 62˚C for 20 min, dewaxed in xylene for 20 min, rehydrated in decreasing concentrations of ethyl alcohol (100, 100, 90, 80 and 70%) for 2 min each followed by boiling in 0.01 M citric acid (pH 6.0)

for 10 min for antigen retrieval. The sections were then incubated in 3% H_2O_2 for 10 min at room temperature to block endogenous peroxidase/phosphatase activity. The sections were blocked with 5% normal goat serum (Thermo Fisher Scientific, Inc.) at room temperature for 15 min, followed by incubation at 4˚C overnight with primary antibodies against rabbit anti-ASF1B (dilution, 1:20; cat. no. ab235358; Abcam) and rabbit anti-Ki67 (dilution, 1:50; cat. no. ab16667; Abcam). A goat anti-rabbit IgG H&L (Alexa Fluor 488) secondary antibody (dilution, 1:100; cat. no. ab150077; Abcam) was used for incubation at 37˚C for 1 h. The color was developed by adding 0.5 ml 3,3'-diaminobenzidine solution for 20 min at room temperature. Images were captured under a light microscope (Eclipse 80i; Nikon Corporation). Ki67-positive cells were counted using ImageJ software (version 5.0; National Institutes of Health).

Apoptotic cells in the tumor tissues were detected using a TUNEL assay kit (Beyotime Institute of Biotechnology). The sections were fixed with 4% paraformaldehyde at 4˚C for 1 h and washed twice with PBS for 20 min at room temperature. The sections were then incubated with 0.5% Triton X-100 and 3% H_2O_2 at room temperature for 10 min followed by incubation with 50 μl TUNEL reaction mixture (5 μl TdT enzyme and 45 μl fluorescent labeling solution) for 1 h at 37˚C in the dark. After three washes with PBS, 1 μg/ml DAPI (Beyotime Institute of Biotechnology) was used for nuclear staining at room temperature for 10 min. The slides were mounted with antifade mounting medium (Wuhan Servicebio Technology Co., Ltd.). Images were captured using a fluorescence microscope (DMI6000B; Leica Microsystems GmbH). Images were captured using a fluorescence microscope (DMI6000B; Leica Microsystems GmbH). Five fields were selected for counting TUNEL-positive cells using ImageJ software (version 5.0; National Institutes of Health).

A HE staining kit (Beyotime Institute of Biotechnology) was used to detect the histology of the harvested tumor tissues. Tissues were fixed with 4% paraformaldehyde for 24 h at room temperature, coated with paraffin and sectioned into 4-μm section. The sections were stained with hematoxylin for 10 min at room temperature followed by incubation with eosin for 30 sec at room temperature. Images were captured under a light microscope (Eclipse 80i; Nikon Corporation).

Statistical analysis. Data are presented as the mean ± SD. *In vitro* data were obtained from three independent experiments. Statistical analyses were performed using GraphPad Prism 7 software (GraphPad Software, Inc.). The paired and unpaired t-test was used for two-group comparisons. One-way ANOVA followed by Tukey's post hoc test and two-way ANOVA followed by Bonferroni's post hoc test were used for multiple-group comparisons. Brown-Forsythe and Bartlett's tests were used to assess the normality and variance homogeneity. The correlation between ASF1B and c-Myc expression was analyzed using the linear regression test. $P<0.05$ was considered to indicate a statistically significant difference.

Results

ASF1B is highly expressed in pancreatic cancer and is closely associated with poor prognosis. To evaluate the potential association between ASF1B and pancreatic cancer, ASF1B expression was analyzed in PAAD samples from TCGA. ASF1B expression was significantly increased in primary tumor samples compared with in normal samples (Fig. 1A). Kaplan-Meier analysis based on the PAAD samples from TCGA revealed that a high level of ASF1B was associated with poor overall survival of patients with pancreatic cancer (Fig. 1B). In the present study, 31 patients with pancreatic cancer were enrolled, and their tumor tissues were collected during surgery. RT-qPCR indicated that ASF1B mRNA expression was significantly higher in pancreatic cancer tissues than in adjacent normal controls (Fig. 1C). Immunohistochemical staining revealed that ASF1B was highly expressed in pancreatic cancer tissues compared with the adjacent normal controls (Fig. 1D). Consistently, ASF1B protein expression was higher in 12 randomly selected pancreatic cancer tissues than in paired adjacent normal controls (Fig. 1E). ASF1B expression was higher in PANC-1 and SW1990 cells than the other three cell lines (Fig. 1F), and thus, these two cell lines were used in subsequent experiments.

Silencing of ASF1B inhibits pancreatic cancer cell proliferation, migration and invasion, and induces apoptosis. Considering that ASF1B is highly expressed in pancreatic cancer, the present study aimed to investigate the effects of ASF1B silencing on pancreatic cancer cells. To this end, two different siRNA sequences specific to ASF1B were transfected into PANC-1 and SW1990 cells. ASF1B protein expression was significantly decreased by ASF1B siRNAs compared with siNC (Fig. 2A). Transfection of PANC-1 and SW1990 cells with ASF1B siRNAs significantly inhibited proliferation (Fig. 2B) and colony formation (Fig. 2C) compared with those of the cells transfected with siNC. Transfection of cells with ASF1B siRNAs significantly increased the apoptosis of PANC-1 and SW1990 cells compared with transfection with siNC (Fig. 2D). In addition, Bax was upregulated and Bcl-2 was downregulated following transfection with ASF1B siRNAs compared with the siNC group (Fig. 2E).

The migration and invasion of PANC-1 and SW1990 cells following transfection with ASF1B siRNAs or siNC were detected using a transwell assay. As shown in Fig. 2F and G, the migration and invasion of PANC-1 and SW1990 cells were significantly inhibited following transfection with ASF1B siRNAs compared with the siNC group. Consistently, ASF1B siRNA transfection significantly inhibited wound healing at 12 h of incubation compared with the siNC group (Fig. 2H and I).

ASF1B induces c-Myc expression in pancreatic cancer cells. Furthermore, the underlying mechanism by which ASF1B exerts its effects on pancreatic cancer cells was explored. GSEA predicted a positive association between ASF1B and the c-Myc signaling pathway (Fig. 3A). The association between ASF1B and the c-Myc signaling pathway was confirmed in subsequent experiments. The mRNA and protein expression levels of c-Myc were downregulated in cells transfected with ASF1B siRNAs compared with siNC (Fig. 3B and C). However, c-Myc protein levels were upregulated in cells transfected with Flag-tagged ASF1B overexpression plasmid compared with the negative control (Fig. 3D). The stability of

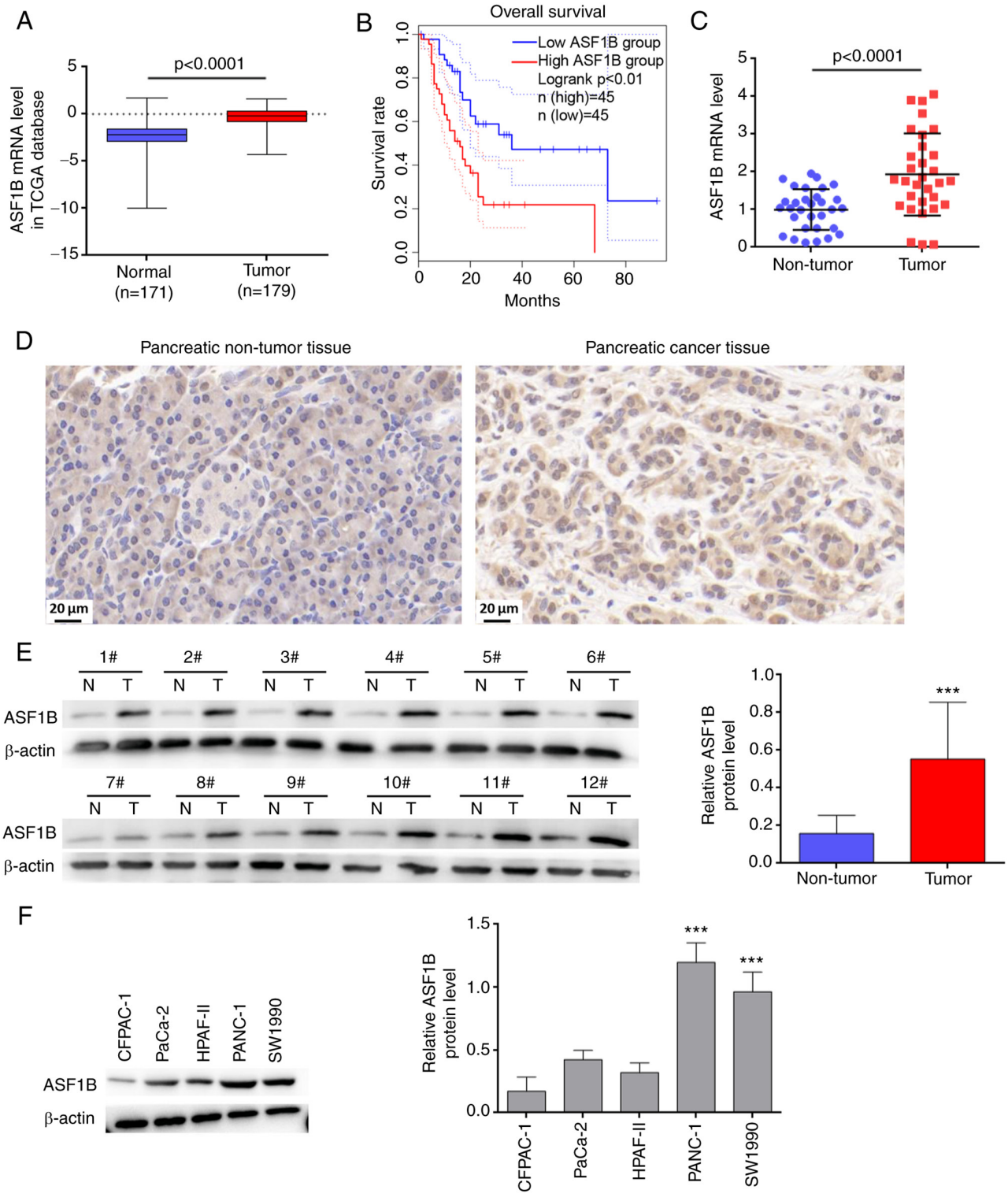

Figure 1. ASF1B is highly expressed in pancreatic cancer and its high expression is closely associated with poor prognosis. (A) ASF1B expression in PAAD samples (n=179) and normal controls (n=171) was analyzed using data from TCGA. (B) Kaplan-Meier analysis based on the PAAD samples from TCGA revealed an association between ASF1B expression and overall survival of patients with pancreatic cancer (n=45 per group). (C) mRNA levels of ASF1B in 31 paired pancreatic cancer and adjacent tissues. (D) Immunohistochemical staining of ASF1B in pancreatic cancer tissues and the paired adjacent normal controls. Scale bar, 20 μm. (E) Protein levels of ASF1B in 12 paired pancreatic cancer and adjacent tissues. ***P<0.001 vs. non-tumor. (F) Protein levels of ASF1B in CFPAC-1, PaCa-2, HPAF-II, PANC-1 and SW1990 cells (n=3). ***P<0.001 vs. CFPAC-1, PaCa-2 and HPAF-II groups. Data in (A) were analyzed using the unpaired t-test. Data in (F) were analyzed using one-way ANOVA followed by Tukey's post hoc test. Other data were analyzed using the paired t-test. ASF1B, anti-silencing function 1B; PAAD, pancreatic adenocarcinoma; TCGA, The Cancer Genome Atlas; N, non-tumor; T, tumor.

c-Myc was detected after treatment with the protein synthesis inhibitor, CHX. As shown in Fig. 3E, ASF1B siRNA regulated c-Myc stability in PANC-1 and SW1990 cells. The protein levels and half-life of c-Myc protein were decreased significantly in the ASF1B siRNA group compared with the siNC group (Fig. 3F and G). Furthermore, a linear regression test

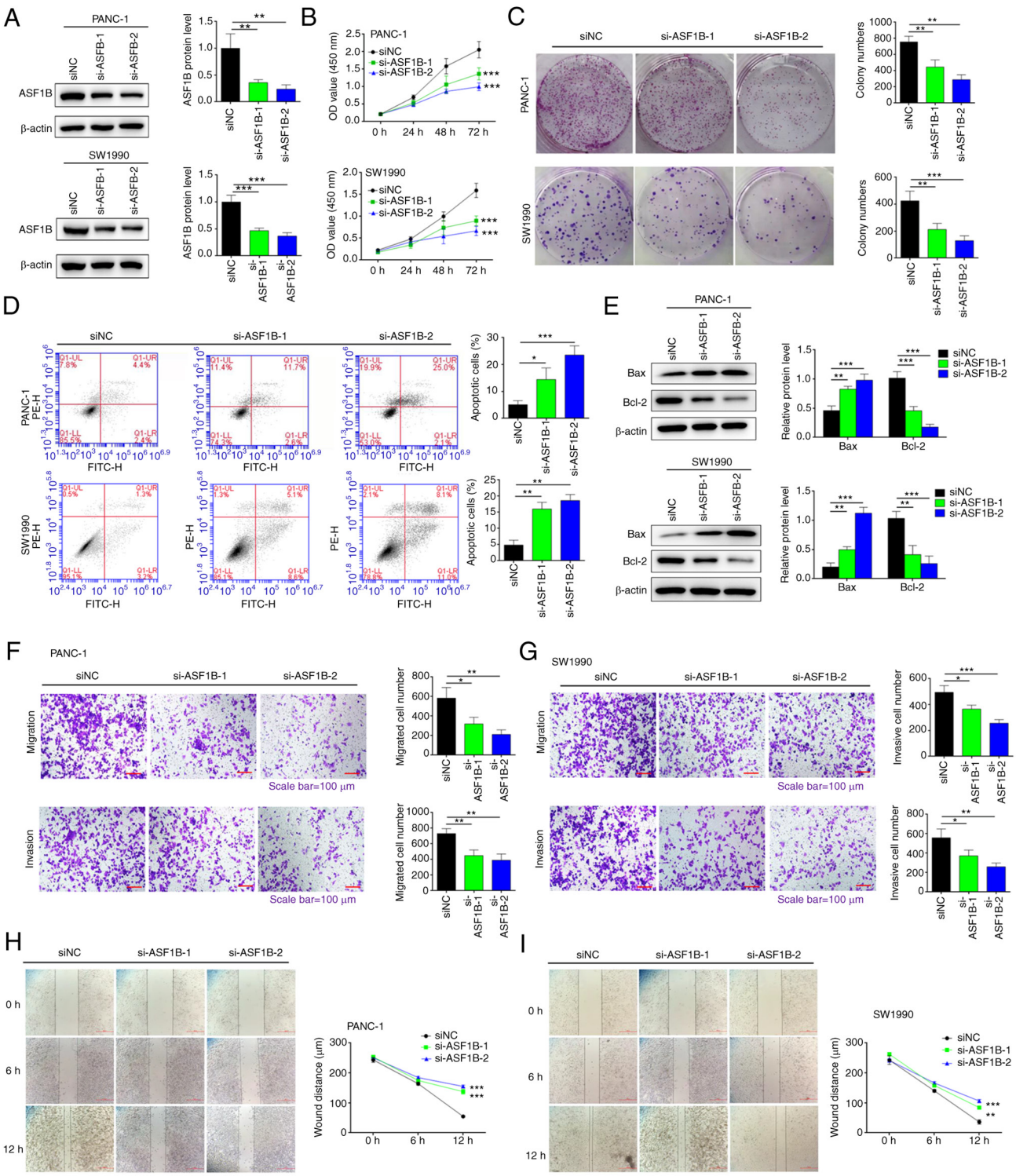

Figure 2. Silencing of ASF1B inhibits pancreatic cancer cell proliferation, migration and invasion, and induces apoptosis. (A) PANC-1 and SW1990 cells were transfected with ASF1B siRNAs (si-ASF1B-1 and si-ASF1B-2) or siNC. Protein levels of ASF1B were measured by western blotting. (B) Cell proliferation, (C) colony formation, (D) apoptosis, and (E) expression levels of Bax and Bcl-2 were detected by Cell Counting Kit-8 assays, colony formation assays, flow cytometry and western blotting, respectively. (F) PANC-1 and (G) SW1990 cells were transfected with ASF1B siRNAs (si-1 and si-2) or siNC. Cell migration and invasion were detected by transwell assays. Magnification, x100; scale bar, 100 μm. The wound distance of (H) PANC-1 and (I) SW1990 cell cultures was detected using a scratch test. Magnification, x40; scale bar, 200 μm. Data are presented as the mean ± SD (n=3). *P<0.05, **P<0.01, ***P<0.001 vs. siNC group. Data in (B) were analyzed using two-way ANOVA followed by Bonferroni's post hoc test. Other data were analyzed using one-way ANOVA followed by Tukey's post hoc test. Brown-Forsythe and Bartlett's tests were used to assess the normality and variance homogeneity. ASF1B, anti-silencing function 1B; NC, negative control; OD, optical density; siRNA/si, small interfering RNA.

revealed a positive correlation between ASF1B and c-Myc mRNA expression in 31 pancreatic cancer tissues (R^2=0.1881; P=0.0148; Fig. 3H).

ASF1B induces c-Myc expression through CBP-mediated H3K56ac. The present study next investigated whether ASF1B upregulates c-Myc expression by inducing H3K56ac.

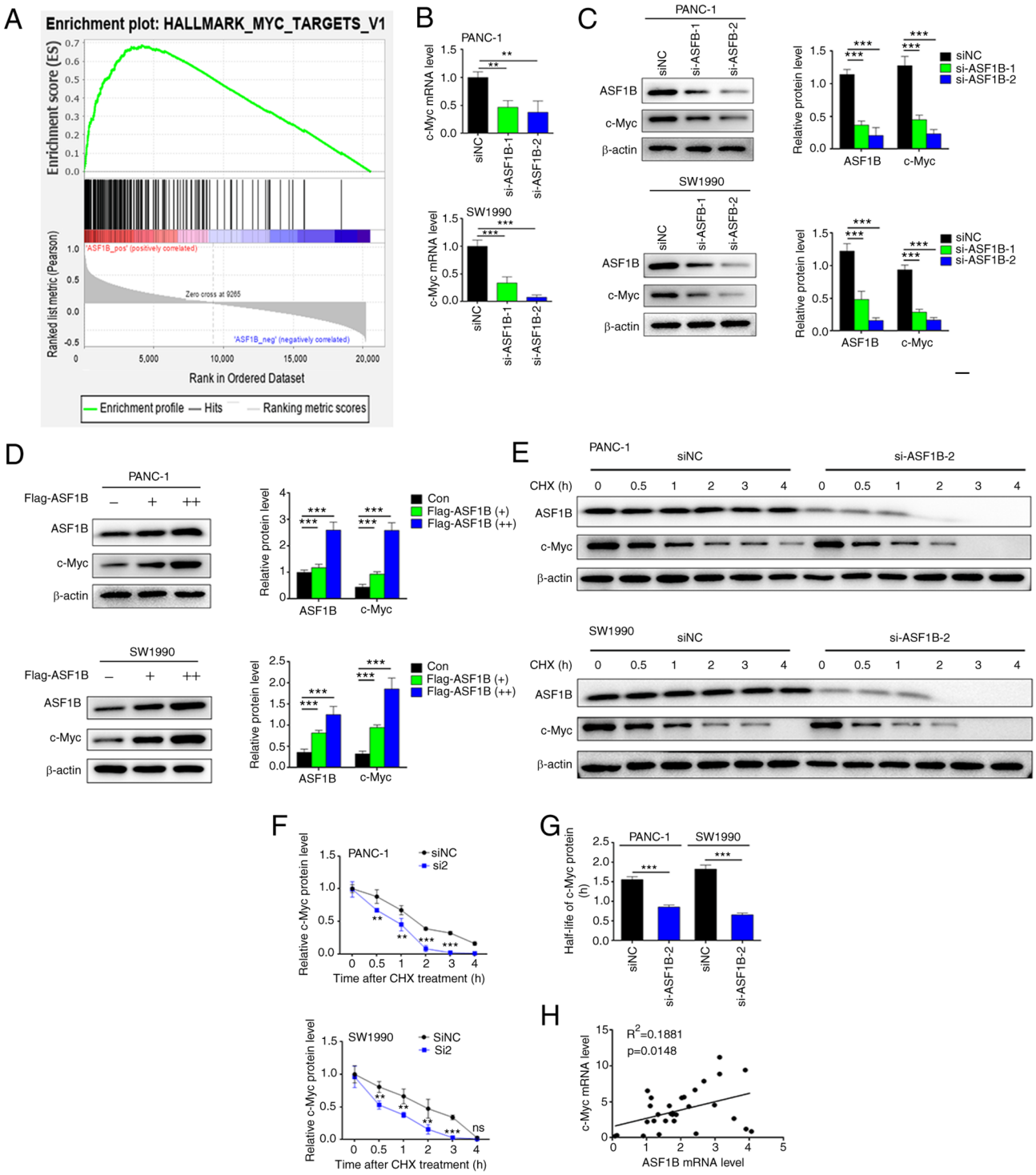

Figure 3. ASF1B induces c-Myc expression in pancreatic cancer cells. (A) Gene Set Enrichment Analysis in pancreatic adenocarcinoma samples from The Cancer Genome Atlas showed the enrichment of c-Myc activation. (B) PANC-1 and SW1990 cells were transfected with ASF1B siRNAs (si-1 and si-2) or siNC. mRNA levels of c-Myc were detected by reverse transcription-quantitative PCR. (C) Protein levels of c-Myc were detected by western blotting. (D) PANC-1 and SW1990 cells were transfected with Flag-tagged ASF1B plasmid. Protein levels of c-Myc were detected by western blotting. Data were analyzed using one-way ANOVA followed by Tukey's post hoc test. Brown-Forsythe and Bartlett's tests were used to assess the normality and variance homogeneity. (E) c-Myc protein stability was detected following treatment with CHX. (F) Relative c-Myc expression. Data were analyzed using two-way ANOVA followed by Bonferroni's post hoc test. (G) Half-life of c-Myc protein. Data were analyzed using the unpaired t-test. (H) A linear regression test revealed the correlation between ASF1B and c-Myc in 31 pancreatic cancer tissues. Data are presented as the mean ± SD (n=3). **P<0.01, ***P<0.001 vs. siNC group. ASF1B, anti-silencing function 1B; CHX, cycloheximide; Con, control (empty vector); NC, negative control; siRNA/si, small interfering RNA.

In PANC-1 and SW1990 cells, silencing of ASF1B by specific siRNAs significantly inhibited the protein levels of acetylated H3K56 (Fig. 4A). Overexpression of ASF1B by transfection with Flag-tagged plasmids increased the expression of acetylated H3K56 (Fig. 4B), indicating that ASF1B is a key regulator of H3K56ac. Silencing of acetyltransferase CBP with specific siRNAs inhibited the expression of acetylated H3K56 and c-Myc induced by ASF1B (Fig. 4C). The proof of successful

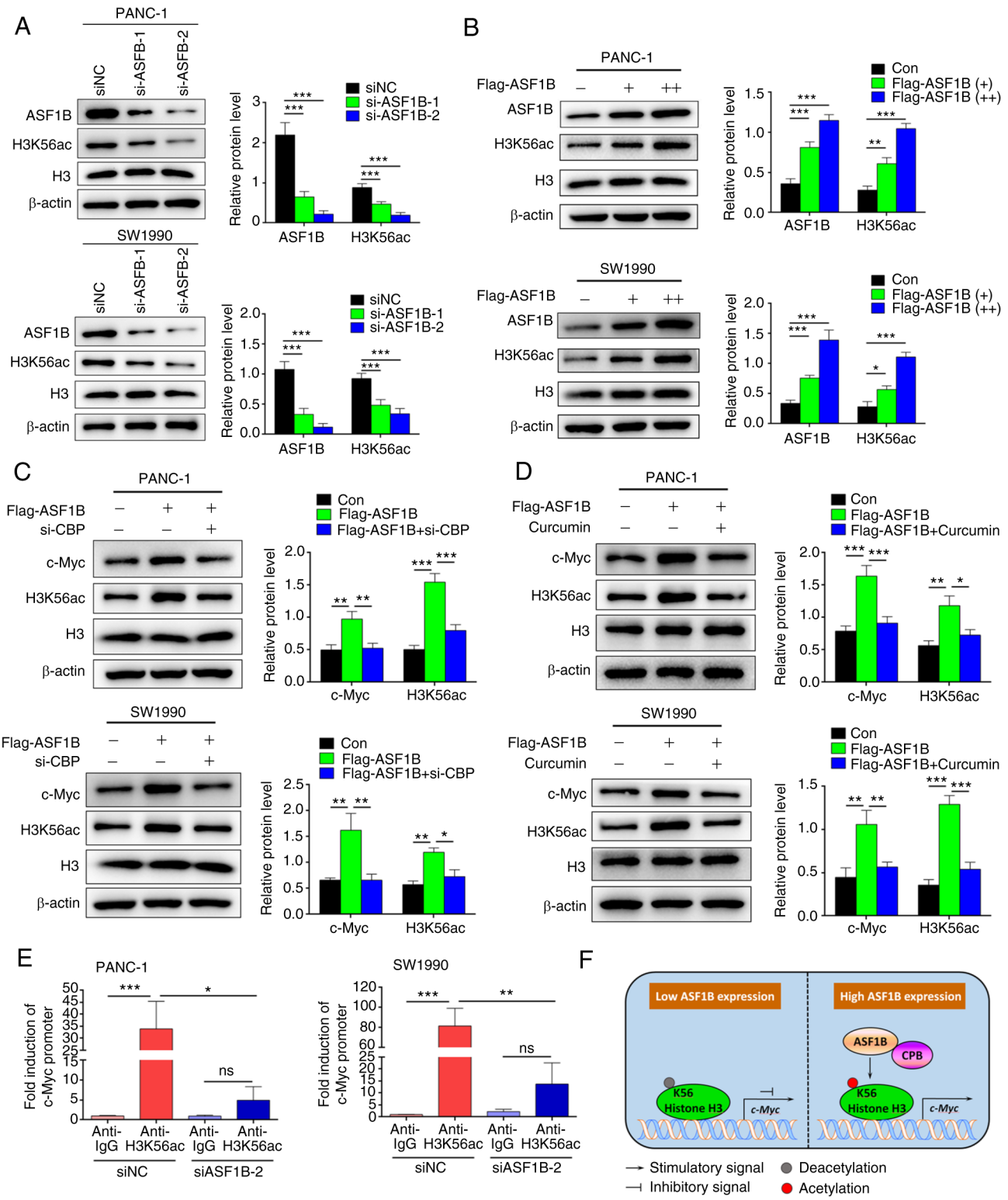

Figure 4. ASF1B induces c-Myc expression through CBP-mediated H3K56 acetylation. The effects of ASF1B (A) silencing and (B) overexpression on H3K56ac were examined by western blotting. The effects of (C) CBP silencing and (D) the CBP inhibitor curcumin on c-Myc and H3K56ac expression were examined by western blotting. (E) Effects of ASF1B on the transcriptional activity of c-Myc were analyzed by chromatin immunoprecipitation. (F) Schematic representation of the proposed mechanism of ASF1B in epigenetic regulation of c-Myc mRNA expression. Data are presented as the mean ± SD (n=3). *P<0.05, **P<0.01, ***P<0.001. Data were analyzed using one-way ANOVA followed by Tukey's post hoc test. Brown-Forsythe and Bartlett's tests were used to assess the normality and variance homogeneity. ASF1B, anti-silencing function 1B; CBP, CREB binding protein; Con, control (empty vector); H3K56ac, histone H3 lysine 56 acetylation; NC, negative control; ns, not significant; siRNA/si, small interfering RNA.

transfection of si-CBP is shown in Fig. S1. Consistently, the CBP inhibitor, curcumin, inhibited the expression of acetylated H3K56 and c-Myc induced by ASF1B (Fig. 4D). The effects of ASF1B on the transcriptional activity of c-Myc were analyzed using ChIP. In siNC transfected PANC-1 and SW1990 cells, 33.9 and 81.4-fold enrichment of the promoter amplification of

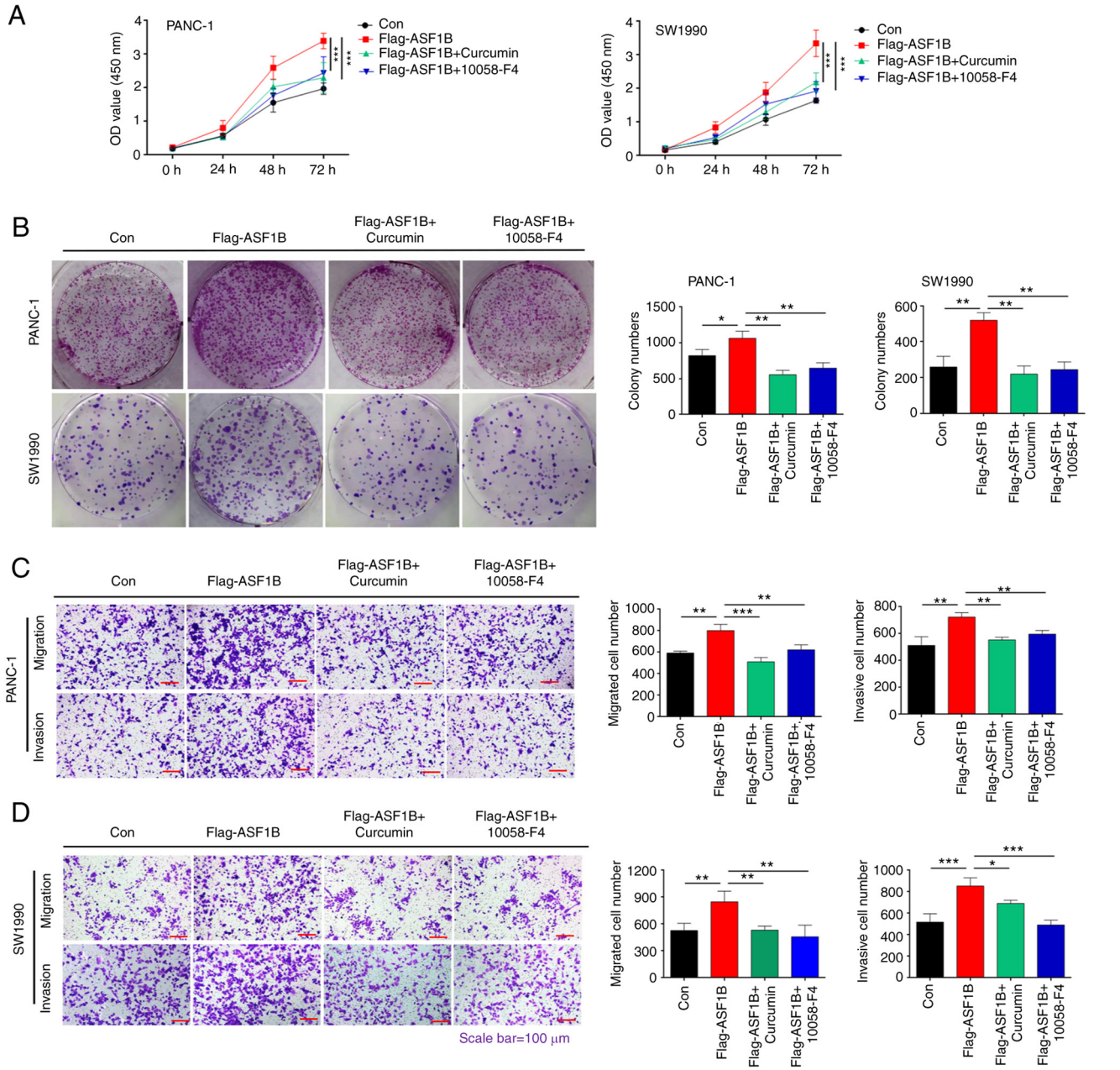

Figure 5. ASF1B promotes pancreatic cancer cell proliferation and metastasis by activating CBP/histone H3 lysine 56 acetylation/c-Myc signaling. (A) PANC-1 and SW1990 cells transfected with ASF1B overexpression plasmid were treated with the CBP inhibitor curcumin or the c-Myc inhibitor 10058-F4. Cell proliferation was detected using Cell Counting Kit-8 assays. (B) Colony formation was detected by colony formation assays. (C) PANC-1 and (D) SW1990 cell migration and invasion were analyzed by transwell assays. Magnification, x100; scale bar, 100 μm. Data are presented as the mean ± SD (n=3). *P<0.05, **P<0.01, ***P<0.001. Data in (A) were analyzed using two-way ANOVA followed by Bonferroni's post hoc test. Other data were analyzed using one-way ANOVA followed by Tukey's post hoc test. Brown-Forsythe and Bartlett's tests were used to assess the normality and variance homogeneity. ASF1B, anti-silencing function 1B; CBP, CREB binding protein; Con, control (empty vector); OD, optical density.

c-Myc was observed using anti-H3K56ac antibodies compared with anti-IgG (Fig. 4E). However, no significant enrichment of the c-Myc promoter was observed in ASF1B-silenced PANC-1 (P=0.847) and SW1990 (P=0.522) cells. These data revealed that ASF1B promoted CBP-mediated H3K56ac to enhance the transcriptional activity of c-Myc in pancreatic cancer cells (Fig. 4F).

ASF1B promotes pancreatic cancer cell proliferation, migration and invasion by activating CBP/H3K56ac/c-Myc signaling. Subsequently, the present study evaluated whether ASF1B contributes to the progression of pancreatic cancer by modulating CBP/H3K56ac/c-Myc signaling *in vitro*. CCK-8 assays revealed that the overexpression of ASF1B enhanced the proliferation of PANC-1 and SW1990 cells, and the CBP inhibitor curcumin and the c-Myc inhibitor 10058-F4 blocked this enhancement (Fig. 5A). In addition, treatment with curcumin and 10058-F4 significantly inhibited the colony formation of PANC-1 and SW1990 cells induced by ASF1B overexpression (Fig. 5B). Transwell assay results demonstrated that migration and invasion induced by ASF1B overexpression in PANC-1 and SW1990 cells were significantly inhibited

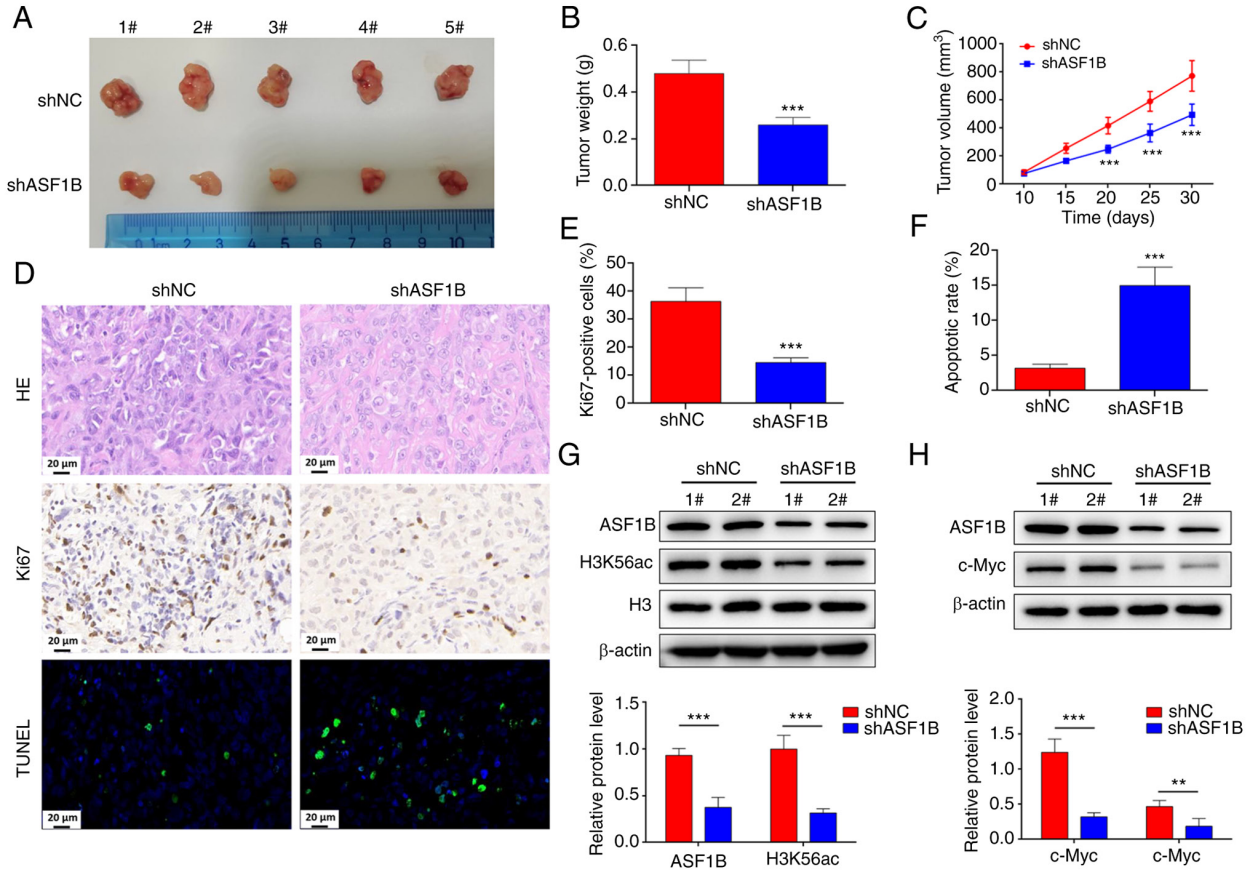

Figure 6. Silencing of ASF1B reduces c-Myc expression and pancreatic cancer growth *in vivo*. (A) A pancreatic cancer xenograft model in BALB/c nude mice was established by injection of PANC-1 cells, which were pre-transfected with shNC or shASF1B. Tumor (B) weight and (C) volume. (D) Representative images of HE staining, Ki-67 immunohistochemical staining and TUNEL staining. (E) Quantification of Ki-67 immunohistochemical staining and (F) TUNEL-positive cells in tumor tissues. (G) H3K56ac and (H) c-Myc protein levels in tumor tissues were detected by western blotting. Data are presented as the mean ± SD (n=5). **P<0.01, ***P<0.001 vs. shNC group. Data in (C) were analyzed using two-way ANOVA followed by Bonferroni's post hoc test. Other data were analyzed using the unpaired t-test. ASF1B, anti-silencing function 1B; H3K56ac, histone H3 lysine 56 acetylation; NC, negative control; sh, short hairpin RNA.

by treatment with curcumin and 10058-F4 (Fig. 5C and D). In summary, these data indicated that ASF1B promoted the progression of pancreatic cancer by activating CBP/H3K56ac/c-Myc signaling *in vitro*.

Silencing of ASF1B reduces c-Myc expression and pancreatic cancer growth in vivo. The present study further determined the role of ASF1B in pancreatic cancer development *in vivo*. Therefore, pancreatic cancer xenografts were established by injecting BALB/c nude mice with PANC-1 cells that were pre-transfected with shNC or shASF1B. The proof of successful transfection of shASF1B is shown in Fig. S2. Compared with those in the shNC group, the mice in the shASF1B group had a lower tumor weight and volume at day 20, 25 and 30 (Fig. 6A-C). HE staining results showed that, compared with the shNC group, the shASF1B group tumor tissues exhibited focal necrosis (Fig. 6D). The percentage of Ki67-positive cells was reduced, and the TUNEL-positive cell rate was increased significantly in the tumor tissues of the shASF1B group (Fig. 6D-F). Furthermore, ASF1B was weakly expressed in the shASF1B group, with low expression of H3K56ac and c-Myc (Fig. 6G and H), indicating that silencing of ASF1B inhibited c-Myc expression and tumor growth *in vivo*.

Discussion

Pancreatic cancer is one of the deadliest malignancies of the digestive system worldwide (32). It has been previously reported that the histone chaperone ASF1B is a biomarker for predicting the outcome of human cancers, including pancreatic cancer (15,33). Silencing of ASF1B influences prostate cancer cell apoptosis by inhibiting PI3K/AKT signaling (11). ASF1B increases migration and growth of clear cell renal cell carcinoma by activating AKT signaling (34). Silencing of ASF1B induces pancreatic cancer cell death and inhibits cancer cell micrometastasis via inactivation of the PI3K/AKT signaling pathway (14,15). By analyzing TCGA, ASF1B was identified to be highly expressed in PAAD samples, and its expression was positively associated with poor survival rate. In the present study, high ASF1B expression was also demonstrated in 31 patients with pancreatic cancer. In PANC-1 and SW1990 cells, ASF1B silencing repressed cell proliferation, migration and invasion, indicating the oncogenic role of ASF1B in pancreatic cancer. In addition, to the best of our knowledge, the present study was the first to demonstrate that ASF1B induced c-Myc expression through CBP-mediated H3K56ac. ASF1B exerted oncogenic effects in pancreatic cancer, possibly through the activation of CBP/H3K56ac/c-Myc signaling.

c-Myc has been recognized as a critical regulator of pancreatic cancer progression (19). Various factors that target c-Myc expression have been demonstrated to be effective in regulating tumor progression. For instance, pescadillo ribosomal biogenesis factor 1 enhances resistance to extra-terminal inhibitors and cell proliferation by increasing c-Myc expression in pancreatic cancer (35). F-box and WD repeat domain containing 7 is a negative modulator of glycolytic metabolism that regulates c-Myc/thioredoxin interacting protein signaling in pancreatic cancer (36). Bromodomain PHD finger transcription factor is critical for transcriptional activation of c-Myc in tumorigenesis (37). Proteasome activator subunit 3 increases pancreatic cancer progression via c-Myc/glycolysis signaling (38). The cooperation of dysregulated KRAS and Myc via inhibition of the type I interferon pathway achieves immune evasion in pancreatic cancer cells (39). The present study revealed that ASF1B was positively associated with c-Myc and that ASF1B promoted c-Myc expression in pancreatic cancer cells. To the best of our knowledge, the present study was the first to demonstrate an association between ASF1B and c-Myc in the development of pancreatic cancer, and presented a novel mechanism of ASF1B-mediated pancreatic cancer involving c-Myc activation.

Epigenetic regulation serves a critical role in cancer development, and histone acetylation modulates cancer-related gene expression (40,41). Histone H3K56ac and histone acetyltransferase CBP are involved in cancer progression. It has been reported that hypoxia-provoked K63-polyubiquitinated herpes virus-associated ubiquitin-specific protease affects CBP-regulated acetylation of H3K56 on the promoters of hypoxia-inducible factor 1α-targeted genes to increase metastasis in tumor progression (42). mTORC2 signaling positively supports H3K56ac to regulate metabolic re-programming in gliomas (43). Chromatin marks on Notch-related enhancers exhibit large-scale variations in H3K56ac upon activation (44). In addition, ASF1B is reportedly essential for regulating H3K56ac and this modification in gene transcription and replication (45,46). Genetic deletion of the H3K56 deacetylase enzyme sirtuin 6 leads to increased c-Myc transcription (47,48). The present study revealed that ASF1B enhanced c-Myc expression by modulating H3K56ac and promoting H3K56ac at the c-Myc promoter. These data revealed a novel mechanism involving ASF1B/CBP/H3K56ac/c-Myc in pancreatic cancer progression.

In conclusion, ASF1B promoted pancreatic cancer progression by activating c-Myc through CBP-mediated H3K56ac. The present findings provide novel insights into the mechanism by which ASF1B modulates pancreatic cancer development via CBP/H3K56ac/c-Myc signaling. Therefore, ASF1B may serve as a potential target for pancreatic cancer therapy.

Acknowledgements

Not applicable.

Funding

The present study was supported by National Natural Science Foundation of China joint fund project (grant no. u1404820), Tackling Key Problems of Science and Technology in Henan Province (grant no. 212102310137) and Henan Medical Science and Technology Research plan project (joint construction) (grant no. lhgj20190628).

Availability of data and material

The datasets used and/or analyzed during the current study are available from the corresponding author on reasonable request.

Authors' contributions

MZha conceived and designed the study. LZ, MZho, EW, and BM performed experiments. QinL, XW, YW, and QioL analyzed and interpreted the data. MZha wrote the manuscript. All authors read and approved the final manuscript. MZha, YW and QioL confirm the authenticity of all the raw data.

Ethics approval and consent to participate

Animal experiments were performed in accordance with the Guide for the Care and Use of Laboratory Animals. Animal and patient experiments were approved by the Ethics Committee of Cancer Hospital Affiliated to Zhengzhou University (Ethics No. 2019-05-006; Zhengzhou, China). This research was conducted under the guidance of the Declaration of Helsinki. All patients provided written informed consent.

Patient consent for publication

Not applicable.

Competing interests

The authors declare that they have no competing interests.

References

1. Siegel RL, Miller KD and Jemal A: Cancer statistics, 2019. CA Cancer J Clin 69: 7-34, 2019.
2. Kamisawa T, Wood LD, Itoi T and Takaori K: Pancreatic cancer. Lancet 388: 73-85, 2016.
3. Kang MJ, Jang JY and Kim SW: Surgical resection of pancreatic head cancer: What is the optimal extent of surgery? Cancer Lett 382: 259-265, 2016.
4. Garrido-Laguna I and Hidalgo M: Pancreatic cancer: From state-of-the-art treatments to promising novel therapies. Nat Rev Clin Oncol 12: 319-334, 2015.
5. Giovannetti E, van der Borden CL, Frampton AE, Ali A, Firuzi O and Peters GJ: Never let it go: Stopping key mechanisms underlying metastasis to fight pancreatic cancer. Semin Cancer Biol 44: 43-59, 2017.
6. Collisson EA, Bailey P, Chang DK and Biankin AV: Molecular subtypes of pancreatic cancer. Nat Rev Gastroenterol Hepatol 16: 207-220, 2019.
7. Ilic M and Ilic I: Epidemiology of pancreatic cancer. World J Gastroenterol 22: 9694-9705, 2016.
8. Mousson F, Ochsenbein F and Mann C: The histone chaperone Asf1 at the crossroads of chromatin and DNA checkpoint pathways. Chromosoma 116: 79-93, 2007.
9. Cote JM, Kuo YM, Henry RA, Scherman H, Krzizike DD and Andrews AJ: Two factor authentication: Asf1 mediates crosstalk between H3 K14 and K56 acetylation. Nucleic Acids Res 47: 7380-7391, 2019.
10. Paul PK, Rabaglia ME, Wang CY, Stapleton DS, Leng N, Kendziorski C, Lewis PW, Keller MP and Attie AD: Histone chaperone ASF1B promotes human β-cell proliferation via recruitment of histone H3.3. Cell Cycle 15: 3191-3202, 2016.

11. Han G, Zhang X, Liu P, Yu Q, Li Z, Yu Q and Wei X: Knockdown of anti-silencing function 1B histone chaperone induces cell apoptosis via repressing PI3K/Akt pathway in prostate cancer. Int J Oncol 53: 2056-2066, 2018.
12. Corpet A, De Koning L, Toedling J, Savignoni A, Berger F, Lemaître C, O'Sullivan RJ, Karlseder J, Barillot E, Asselain B, *et al*: Asf1b, the necessary Asf1 isoform for proliferation, is predictive of outcome in breast cancer. EMBO J 30: 480-493, 2011.
13. Rosty C, Sheffer M, Tsafrir D, Stransky N, Tsafrir I, Peter M, de Crémoux P, de La RA, Salmon R, Dorval T, *et al*: Identification of a proliferation gene cluster associated with HPV E6/E7 expression level and viral DNA load in invasive cervical carcinoma. Oncogene 24: 7094-7104, 2005.
14. Kim JH, Youn Y, Lee JC, Kim J, Ryu JK and Hwang JH: Downregulation of ASF1B inhibits tumor progression and enhances efficacy of cisplatin in pancreatic cancer. Cancer Biomark 34: 647-659, 2022.
15. Wang K, Hao Z, Fu X, Li W, Jiao A and Hua X: Involvement of elevated ASF1B in the poor prognosis and tumorigenesis in pancreatic cancer. Mol Cell Biochem 477: 1947-1957, 2022.
16. Thomas LR, Foshage AM, Weissmiller AM and Tansey WP: The MYC-WDR5 nexus and cancer. Cancer Res 75: 4012-4015, 2015.
17. Pelengaris S and Khan M: The c-MYC oncoprotein as a treatment target in cancer and other disorders of cell growth. Expert Opin Ther Targets 7: 623-642, 2003.
18. Dang CV: MYC on the path to cancer. Cell 149: 22-35, 2012.
19. Hessmann E, Schneider G, Ellenrieder V and Siveke JT: MYC in pancreatic cancer: Novel mechanistic insights and their translation into therapeutic strategies. Oncogene 35: 1609-1618, 2016.
20. Wirth M, Mahboobi S, Kramer OH and Schneider G: Concepts to target MYC in pancreatic cancer. Mol Cancer Ther 15: 1792-1798, 2016.
21. Hogg SJ, Beavis PA, Dawson MA and Johnstone RW: Targeting the epigenetic regulation of antitumour immunity. Nat Rev Drug Discov 19: 776-800, 2020.
22. Chen Y, Hong T, Wang S, Mo J, Tian T and Zhou X: Epigenetic modification of nucleic acids: From basic studies to medical applications. Chem Soc Rev 46: 2844-2872, 2017.
23. Dawson MA and Kouzarides T: Cancer epigenetics: From mechanism to therapy. Cell 150: 12-27, 2012.
24. Audia JE and Campbell RM: Histone modifications and cancer. Cold Spring Harb Perspect Biol 8: a019521, 2016.
25. Liu Z, Yang L, Sun Y, Xie X and Huang J: ASF1a enhances antiviral immune response by associating with CBP to mediate acetylation of H3K56 at the Ifnb promoter. Mol Immunol 78: 57-64, 2016.
26. Zhang L, Serra-Cardona A, Zhou H, Wang M, Yang N, Zhang Z and Xu RM: Multisite substrate recognition in asf1-dependent acetylation of histone H3 K56 by Rtt109. Cell 174: 818-830.e811, 2018.
27. Shaukat A, Khan MHF, Ahmad H, Umer Z and Tariq M: Interplay between BALL and CREB binding protein maintains H3K27 acetylation on active genes in drosophila. Front Cell Dev Biol 9: 740866, 2021.
28. Das C, Lucia MS, Hansen KC and Tyler JK: CBP/p300-mediated acetylation of histone H3 on lysine 56. Nature 459: 113-117, 2009.
29. Tang Z, Kang B, Li C, Chen T and Zhang Z: GEPIA2: An enhanced web server for large-scale expression profiling and interactive analysis. Nucleic Acids Res 47: W556-W560, 2019.
30. Yu G, Wang LG, Han Y and He QY: clusterProfiler: An R package for comparing biological themes among gene clusters. OMICS 16: 284-287, 2012.
31. Livak KJ and Schmittgen TD: Analysis of relative gene expression data using real-time quantitative PCR and the 2(-Delta Delta C(T)) method. Methods 25: 402-408, 2001.
32. Siegel RL, Miller KD and Jemal A: Cancer statistics, 2017. CA Cancer J Clin 67: 7-30, 2017.
33. Hu X, Zhu H, Zhang X, He X and Xu X: Comprehensive analysis of pan-cancer reveals potential of ASF1B as a prognostic and immunological biomarker. Cancer Med 10: 6897-6916, 2021.
34. Jiangqiao Z, Tao Q, Zhongbao C, Xiaoxiong M, Long Z, Jilin Z and Tianyu W: Anti-silencing function 1B histone chaperone promotes cell proliferation and migration via activation of the AKT pathway in clear cell renal cell carcinoma. Biochem Biophys Res Commun 511: 165-172, 2019.
35. Jin X, Fang R, Fan P, Zeng L, Zhang B, Lu X and Liu T: PES1 promotes BET inhibitors resistance and cells proliferation through increasing c-Myc expression in pancreatic cancer. J Exp Clin Cancer Res 38: 463, 2019.
36. Jensen MB, Lawaetz JG, Andersson AM, Petersen JH, Nordkap L, Bang AK, Ekbom P, Joensen UN, Prætorius L, Lundstrøm P, *et al*: Vitamin D deficiency and low ionized calcium are linked with semen quality and sex steroid levels in infertile men. Hum Reprod 31: 1875-1885, 2016.
37. Richart L, Carrillo-de Santa Pau E, Rio-Machin A, de Andrés MP, Cigudosa JC, Lobo VJ and Real FX: BPTF is required for c-MYC transcriptional activity and in vivo tumorigenesis. Nat Commun 7: 10153, 2016.
38. Guo J, Hao J, Jiang H, Jin J, Wu H, Jin Z and Li Z: Proteasome activator subunit 3 promotes pancreatic cancer growth via c-Myc-glycolysis signaling axis. Cancer Lett 386: 161-167, 2017.
39. Muthalagu N, Monteverde T, Raffo-Iraolagoitia X, Wiesheu R, Whyte D, Hedley A, Laing S, Kruspig B, Upstill-Goddard R, Shaw R, *et al*: Repression of the type I interferon pathway underlies MYC- and KRAS-dependent evasion of NK and B cells in pancreatic ductal adenocarcinoma. Cancer Discov 10: 872-887, 2020.
40. Okugawa Y, Grady WM and Goel A: Epigenetic alterations in colorectal cancer: Emerging biomarkers. Gastroenterology 149: 1204-1225 e1212, 2015.
41. Benton CB, Fiskus W and Bhalla KN: Targeting histone acetylation: Readers and writers in leukemia and cancer. Cancer J 23: 286-291, 2017.
42. Wu HT, Kuo YC, Hung JJ, Huang CH, Chen WY, Chou TY, Chen Y, Chen YJ, Chen YJ, Cheng WC, *et al*: K63-polyubiquitinated HAUSP deubiquitinates HIF-1alpha and dictates H3K56 acetylation promoting hypoxia-induced tumour progression. Nat Commun 7: 13644, 2016.
43. Vadla R and Haldar D: Mammalian target of rapamycin complex 2 (mTORC2) controls glycolytic gene expression by regulating histone H3 Lysine 56 acetylation. Cell Cycle 17: 110-123, 2018.
44. Skalska L, Stojnic R, Li J, Fischer B, Cerda-Moya G, Sakai H, Tajbakhsh S, Russell S, Adryan B and Bray SJ: Chromatin signatures at Notch-regulated enhancers reveal large-scale changes in H3K56ac upon activation. EMBO J 34: 1889-1904, 2015.
45. Weng M, Yang Y, Feng H, Pan Z, Shen WH, Zhu Y and Dong A: Histone chaperone ASF1 is involved in gene transcription activation in response to heat stress in Arabidopsis thaliana. Plant Cell Environ 37: 2128-2138, 2014.
46. Han J, Zhou H, Li Z, Xu RM and Zhang Z: Acetylation of lysine 56 of histone H3 catalyzed by RTT109 and regulated by ASF1 is required for replisome integrity. J Biol Chem 282: 28587-28596, 2007.
47. Sebastián C, Zwaans BM, Silberman DM, Gymrek M, Goren A, Zhong L, Ram O, Truelove J, Guimaraes AR, Toiber D, *et al*: The histone deacetylase SIRT6 is a tumor suppressor that controls cancer metabolism. Cell 151: 1185-1199, 2012.
48. Cai J, Zuo Y, Wang T, Cao Y, Cai R, Chen FL, Cheng J and Mu J: A crucial role of SUMOylation in modulating Sirt6 deacetylation of H3 at lysine 56 and its tumor suppressive activity. Oncogene 35: 4949-4956, 2016.